

A BASIC ANALYSIS ABOUT INDUCED EMF OF PLANAR COILS TO RING COILS

E. M. M. Costa

Universidade Federal do Vale do São Francisco — UNIVASF
Colegiado de Engenharia Elétrica — CENEL
Av. Antônio Carlos Magalhães, 510, Juazeiro, BA, Brazil

Abstract—This paper presents a basic analysis about the results of experiments using planar coils inner to ring coils, when planar coil is applied to a square wave voltage. In this study an uncommon phenomenon occurs in the ring coil, which is analyzed.

1. INTRODUCTION

In existent literature about planar coils, several works are developed on microcircuits [1–8], which the analyzed effects are based on sinusoidal voltages [9–14, 30]. When analyzing coil's inductance, some papers present results of the existence of parasitic capacitances (stray capacitances) [15–17], that interfere with the system on several aspects, as transformers [18–21]. In these researches, evaluations about effects of parasitic capacitances in planar coils and ring coils with diameters greater than 2 cm, as response of the induced *emf* in the ring coil when a step voltage excites the primary are not found. Little is found in researches about effects of square waves in coils, where most researches of square waves is applied to power electronics [22–25] or others [26–29].

This paper presents some experimental results about observed effects in systems defined by planar coil *vs* ring coil, where the planar coil presents 200 turns fixed; this planar coil is considered as the primary of an air core transformer; the ring coil is the secondary of this transformer, which has the turn number varying on worked experiments. The results are presented in this paper.

This paper is formalized as follows. In Section 2, the data of the used equipments and coils are presented. In Section 3, the experimental results are presented and analyzed, describing some explanations of

Corresponding author: E. M. M. Costa (eduard.montgomery@univasf.edu.br).

the phenomena governing the found effects. In Section 4, some observations about the phenomena are discussed. Section 5 presents the conclusions.

2. PRIMARY DATA OF THE SYSTEM IN ANALYSIS

In the realized experiments in this work, several concentric coils were used, forming an air core transformer, being the primary of the transformer, a planar coil with 200 turns copper wire with diameter 2.02×10^{-4} m (32 AWG) and the secondary formed by a ring coil. The primary coil (planar coil) presents a diameter $d = 4.01 \times 10^{-2}$ m with the copper wires bunched together on layers with height $h = 5 \times 10^{-4}$ m. The secondary of this transformer uses coils with turn number $n = 2, 5, 7, 9, 10, 12, 15, 20, 30$ and 50, respectively, where the coils of 5 and 20 turns were constructed by copper wire of diameter 2.02×10^{-4} m (32 AWG), while the others were constructed by copper wire of diameter 1.80×10^{-4} m (36 AWG). These ring coils present turn diameter $D = 4.65 \times 10^{-2}$ m arranged such that their heights are the same as that of the planar coil in the primary of the transformer. Each coil has a resistance due to the total length of the wire, a specific inductance, a specific capacitance, and each ring coil presents a mutual inductance on the primary planar coil. These data appear in Table 1; considering that the resistance was measured, and the inductance L was calculated

Table 1. Coils' data.

n	r (Ω)	L (H)	C (F)	d (m)	M
2 (ring)	0.8	1.72×10^{-7}	8.24×10^{-10}	1.8×10^{-4}	2.18×10^{-5}
5 (ring)	0.62	1.69×10^{-7}	3.68×10^{-9}	2.02×10^{-4}	5.45×10^{-5}
7 (ring)	1.81	1.72×10^{-7}	4.94×10^{-9}	1.8×10^{-4}	7.64×10^{-5}
9 (ring)	2.2	1.72×10^{-7}	6.59×10^{-9}	1.8×10^{-4}	9.82×10^{-5}
10 (ring)	2.48	1.72×10^{-7}	7.41×10^{-9}	1.8×10^{-4}	1.091×10^{-4}
12 (ring)	2.8	1.72×10^{-7}	9.06×10^{-9}	1.8×10^{-4}	1.309×10^{-4}
15 (ring)	3.49	1.72×10^{-7}	1.15×10^{-8}	1.8×10^{-4}	1.6364×10^{-4}
20 (ring)	1.73	1.69×10^{-7}	1.75×10^{-8}	2.02×10^{-4}	2.182×10^{-4}
30 (ring)	6.78	1.72×10^{-7}	2.39×10^{-8}	1.8×10^{-4}	2.373×10^{-4}
50 (ring)	11.1	1.72×10^{-7}	4.04×10^{-8}	1.8×10^{-4}	5.455×10^{-4}
200 (planar)	77.4	1.65×10^{-7}	9.21×10^{-10}	2.02×10^{-4}	–

through equation [31]:

$$L = \mu_0 \frac{D}{2} \left(\ln \left(\frac{8D}{d} \right) - \frac{7}{4} \right) \quad (1)$$

where D is the mean diameter of the ring coil; d is the wire's diameter; the parasitic capacitances (C_{gi} — ground capacitance and C_{ti} — turn to turn coil capacitance, $i = 1, 2$) were calculated through equations of [15]; the mutual inductances on planar coil M were calculated through equation [32]:

$$M = \frac{1}{2} \mu_0 \sqrt{(a+b)^2 + z^2} ((2-m)K(m) - 2E(m)) \quad (2)$$

$$m = \frac{4ab}{(a+b)^2 + z^2} \quad (3)$$

where a and b are the coils' radii; z is its distance; $K(m)$ and $E(m)$ are complete elliptical integrals of first and second kinds [33], respectively.

Also, the measurement of the capacitance inter two coils (planar *vs* ring) presents the value of $C_{pr} = 3.1 \times 10^{-11}$ F.

The equipments used in these experiments were a digital storage oscilloscope Agilent Technologies DSO3202A with passive probe N2862A (input resistance = 10 M Ω and input capacitance \simeq 12 pF), a function generator Rigol DG2021A and a digital multimeter Agilent Technologies U1252A.

Figure 1 shows the basic structure of the system in analysis (planar coil inner ring coil), where the experiments were realized. In these experiments, the square wave excites planar coil considering ground as the edge of the disc, and positive voltage as the wire in center, to observe the phenomena that will be described. Otherwise, output signals are different, similar to the situation that will be described at the end of Section 4.

The initial experiments were realized with an excitation of the primary (planar coil) based on a square wave of 5 V_{pp} (2.5 V_{max}), with frequencies ranging from 1 kHz and 300 kHz, observing the responses of the secondary open circuit (ring coil).

The experimental data obtained in this configuration, a priori, were sufficient to determine several effects not common, which are described in the next sections.

3. EXPERIMENTS AND INFORMATION'S EXTRACTION

Considering the described system, when exciting by low frequency square wave (in planar coil), the ring coil generates an output response

similar to step voltage, showing the same response.

To understand the phenomenon in these experiments, we initially consider the secondary coil as a ring coil with 10 turns, and the planar coil excited with a signal voltage based on square wave of frequency $f = 1$ kHz. In this case, the signal response of the ring coil presents as Faraday's law:

$$emf = -\frac{d\Phi}{dt} \quad (4)$$

that we can observe in Fig. 2, where input signal is shown in upper graph (effect of RL circuit excited by a square wave), and lower graph is the signal response of the ring coil. In this case, the response signal in ring coil has positive signal on input planar coil, because the passive

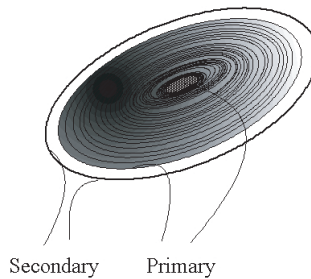


Figure 1. Air core transformer with planar coil of 200 turns as primary and ring coil as secondary.

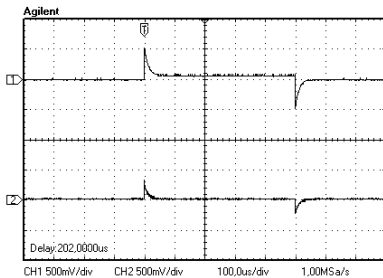


Figure 2. Input in primary planar coil with $f = 1$ kHz square wave and output according to Faraday's law: inverted connection of ring coil to oscilloscope to warranty same relation with input.

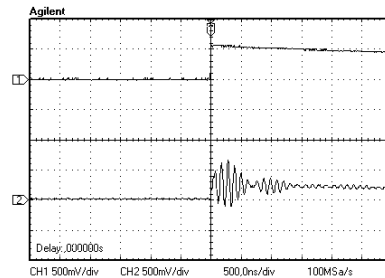


Figure 3. Time expansion in oscilloscope to 500.0 ns/div and information's extraction from the output signal response.

probe was inverted for the convenience of analyzing the system.

However, extending the viewing time of the signal in oscilloscope for 500.0 ns/div (that is shown in Fig. 3), we note that the output signal shows a variation of a double sine wave, with lower frequency ($f_{10<}$) modulating at higher frequency ($f_{10>}$), where the index 10 refers to the number of turns of the used ring coil. Removing the values of these frequencies for the case of this first experiment, we find approximately the values of:

$$\begin{aligned} f_{10>} &= 8.3333 \text{ MHz} \\ f_{10<} &= 714.285 \text{ kHz} \end{aligned}$$

from the periods found in this graph. In this case, we find that the system has a response to the input step voltage, extracted from graphic of the Fig. 3, approximately given by:

$$V_0 = - \left[\sin(52,359,668.12t) \sin(4,487,985.92t) e^{-3.4 \times 10^6 t} + 0.35 \right] e^{-1.25 \times 10^5 t} \quad (5)$$

Noting in the same Fig. 3, we see that in the input signal, minimal variations are found. Using Faraday's law on Equation (4), we find that the variable magnetic flux is given by:

$$\begin{aligned} \Phi(t) &= - \int emf dt \\ \Phi(t) &= -7.649 \times 10^{-10} \cos(47,871,682.2t) e^{-3.525 \times 10^6 t} + \\ &+ 1.04 \times 10^{-8} \sin(47,871,682.2t) e^{-3.525 \times 10^6 t} + \\ &+ 5.43 \times 10^{-10} \cos(56,847,654.04t) e^{-3.525 \times 10^6 t} - \\ &- 8.76 \times 10^{-9} \sin(56,847,654.04t) e^{-3.525 \times 10^6 t} + \\ &- 2.8 \times 10^{-6} e^{-1.25 \times 10^5 t} \end{aligned} \quad (6)$$

which is caused by the current in the planar coil when excited by step voltage (rise effect of the square wave voltage), which is almost imperceptible in the upper graph of Fig. 3.

Considering the other ring coils, we find the graphs in Fig. 4.

For these graphs, we can see that the frequencies are approximately:

$$\begin{aligned} f_{2>} &= 35.714 \text{ MHz} \\ f_{2<} &= 5.0 \text{ MHz} \\ f_{5>} &= 16.667 \text{ MHz} \\ f_{5<} &= 2.976 \text{ MHz} \end{aligned}$$

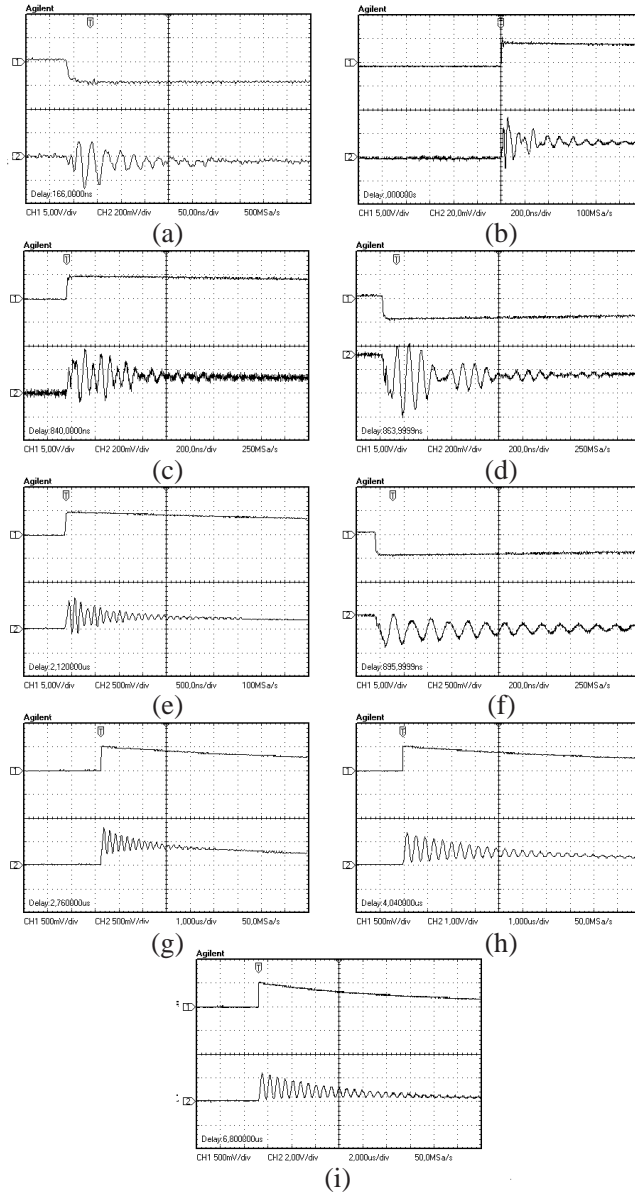


Figure 4. Response of the ring coil to: (a) 2 turns; (b) 5 turns; (c) 7 turns; (d) 9 turns; (e) 12 turns; (f) 15 turns; (g) 20 turns; (h) 30 turns and (i) 50 turns.

$$\begin{aligned}
 f_{7>} &= 14.70588 \text{ MHz} \\
 f_{7<} &= 2.27273 \text{ MHz} \\
 f_{9>} &= 9.259 \text{ MHz} \\
 f_{9<} &= 961.539 \text{ kHz} \\
 f_{12>} &= 7.692 \text{ MHz} \\
 f_{15>} &= 7.143 \text{ MHz} \\
 f_{20>} &= 4.545 \text{ MHz} \\
 f_{30>} &= 2.778 \text{ MHz} \\
 f_{50>} &= 1.389 \text{ MHz}
 \end{aligned}$$

We observe in these graphs, which in ring coils with few turns, the frequencies increases considerably. When increasing the turn number, frequencies decreases, until the effect of modulation becomes non-visible. This effect is visible from ring coil with 12 turns, where the lower frequency, which modulates the higher frequency, reduces its amplitude considerably, presenting as AM-DSB modulation, but with a frequency which cannot be extracted from the graph. Over 15 turns, lower frequency is imperceptible, which is visible only at exponential variation over higher frequency.

All graphs in Fig. 4 are repeated until square wave frequency $f = 300 \text{ kHz}$, when other effects appear, which are analyzed and will be discussed in another paper.

As the induced *emf* shows these variations, we observe that the current in planar coil (primary) that generates the variable magnetic flux has the same variation, being more or less, according to the turn number in ring coil (secondary). According to [15–17], parasitic capacitances are found in coils, such that both the primary and secondary circuits present as *RLC* circuits response to step voltage. Also, because the frequency response of the secondary circuit is much higher than the exciting frequency voltage in primary planar coil, no variation in system's response is verified, which remains as a response to an input step voltage of 2.5 V peak.

4. OBSERVATIONS ABOUT EXPERIMENTS

Looking for flux in Equation (3), which is generated by circulating current in the primary circuit in response to input step voltage, we see that the system presents a characteristic of weak damping *RLC* circuit, which is almost imperceptible in the oscilloscope. This property of the planar coil can be analyzed in relation to parasitic capacitances [15–17], so that the circuit can be made as shown in Fig. 5, where M is the mutual inductance, L_i the self inductance of the coils, r_i their resistances, C_{gi}

the parasitic capacitances in relation to a ground, and C_{ci} turn to turn parasitic capacitances ($i = 1, 2$), v_i the input signal and v_0 the output signal.

Because of the values of parasitic capacitance, inductance and resistance of the coil, the circuit responds to the input step voltage as a weak damping RLC circuit. Furthermore, the effect of capacitances between planar and ring coils, mutual inductance, parasitic capacitances and the self inductance of the ring coil, the double frequency (modulated frequency) found in the response of the variable flux is observed, which creates the effect of induced *emf*.

We can see that such effects are highly visible as response of ring coils with small turn number, where we see the best visibility of these effects in 10 turns ring coil.

The observed frequencies in graphs of Fig. 2, Fig. 3 and Fig. 4 define the graph of Fig. 6, which is formalized as function of the turn number of the ring coil.

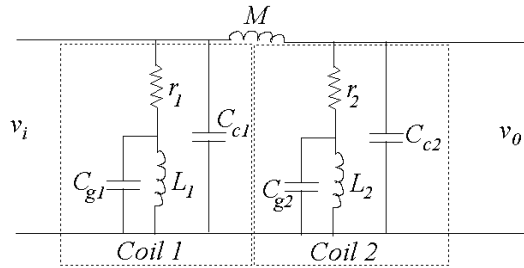


Figure 5. Equivalent circuit of the system, considering coils' resistance and parasitic capacitances.

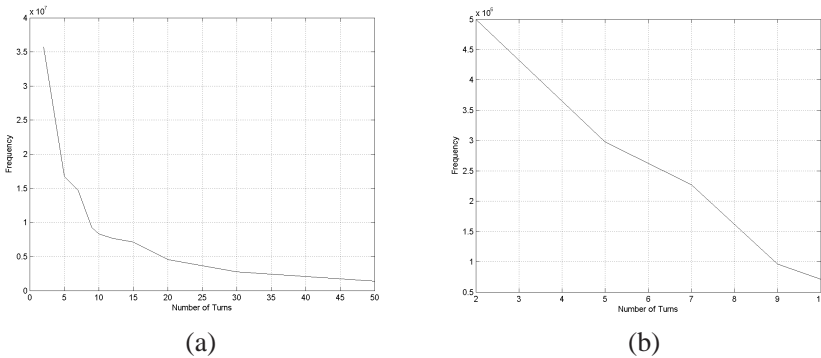


Figure 6. Graphic: (a) n vs $f_{n>}$; (b) n vs $f_{n<}$.

In these graphs we find that the frequency $f_{n>}$ decreases quickly with the turn number n , where we see that this frequency is inversely proportional to the turn number, which relates directly to the inverse proportionality of the parasitic capacitances, the self inductance and mutual inductance:

$$f_{n>} \simeq \frac{7.1428 \times 10^7}{n} \tag{7}$$

This approach is shown in Fig. 7, where the errors are significant, but it is due partly from diameter of copper wire used, which we can see in the previous section. In the case of frequency $f_{n<}$, the relation is almost linear, as seen in Fig. 6(b).

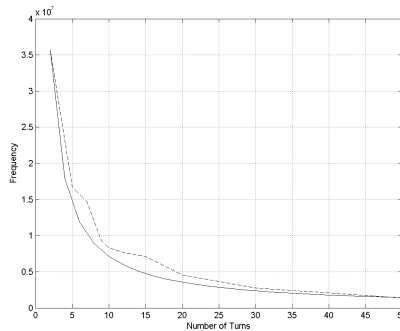


Figure 7. Comparative Graphic n vs $f_{n>}$ and graph function $f_{n>} \simeq \frac{7.1428 \times 10^7}{n}$.

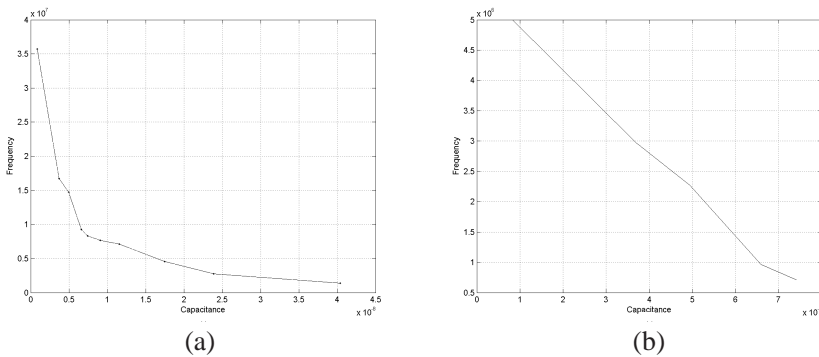


Figure 8. Graphic: (a) ring coil parasitic capacitance vs $f_{n>}$; (b) ring coil parasitic capacitance vs $f_{n<}$.

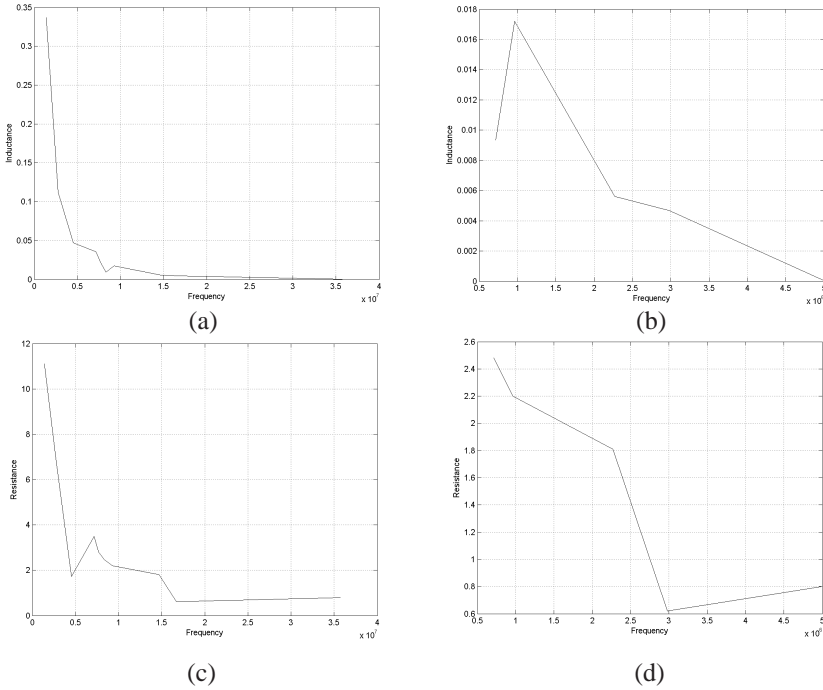


Figure 9. Graphics: (a) $f_{n>}$ vs ring coil inductance; (b) $f_{n<}$ vs ring coil inductance; (c) $f_{n>}$ vs ring coil resistance; (d) $f_{n<}$ vs ring coil resistance.

Similarly, considering the calculation of the parasitic capacitances according to Table 1, we find the graphs shown in Fig. 8, showing similarities with the graphs of Fig. 6.

Verifying graphs of frequencies vs inductances and frequencies vs resistances of the ring coils, we observe some discontinuities since used wires which construct these coils varied in some cases, presenting different diameters, which is observed at specific points of graphics shown in Fig. 9. We can observe that these graphs have a similarity with graphs in Fig. 6, although the visible errors are large on points where diameter of copper wire is 2.02×10^{-4} m.

Also, there are two exponential terms in the ring coil response, whose values should be the response to the exponential drop in predominant primary circuit RL ($\alpha = 1.25 \times 10^5$) and exponential drop specific of the sinusoidal variations when considering the parasitic capacitance ($\alpha = 3.525 \times 10^6$).

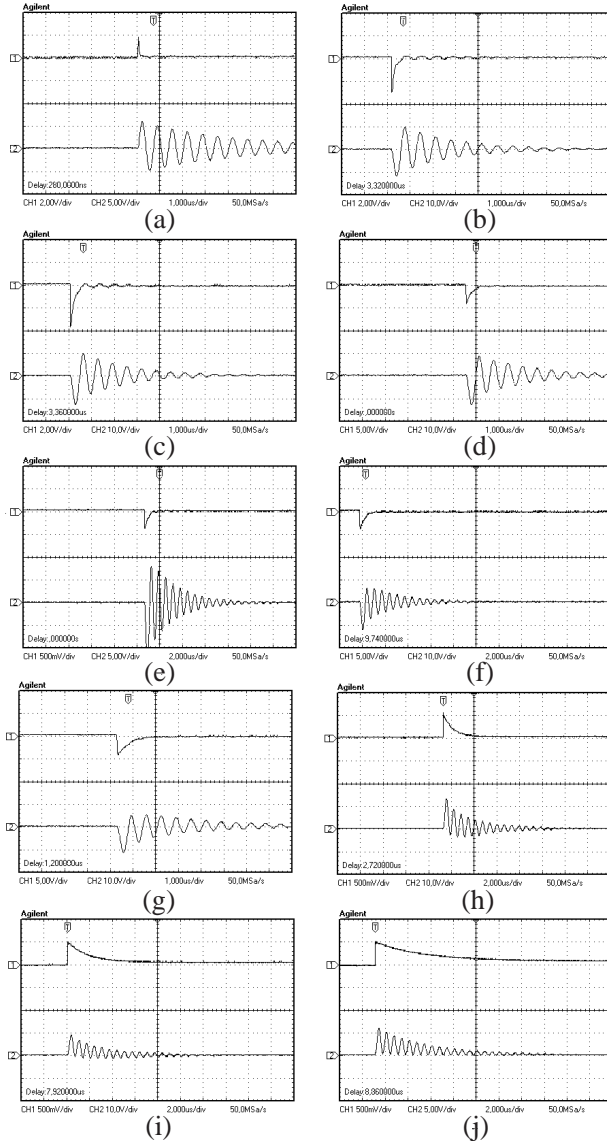


Figure 10. Responses of the inverted system (ring coil *vs* planar coil): (a) Ring coil with 2 turns; (b) Ring coil with 5 turns; (c) Ring coil with 7 turns; (d) Ring coil with 9 turns; (e) Ring coil with 10 turns; (f) Ring coil with 12 turns; (g) Ring coil with 15 turns; (h) Ring coil with 20 turns; (i) Ring coil with 30 turns and (j) Ring coil with 50 turns.

However, when the system is reversed, i.e., the planar coil is defined as the secondary, and ring coil is excited as the primary. The response of the system for any number of turns in the ring coil is always similar to the graphs of Fig. 4 (for the turn number greater than 12 turns). A priori, we observe in this case that for an input square wave, the response of the ring coil has some variations, but the planar coil maintains an oscillation with exponential decrease, independent of the turn number in the ring coil. These cases are shown in Fig. 10.

In this inversion between the primary and the secondary we note that the increase of the number of turns generates a reduction in observed variation in primary coil (ring) as well a different effect in secondary response (planar coil), that is a elimination of the symmetry, which is due to increased inductance and the parasitic capacitance of the circuit connected as a whole (effect of inversion of capacitances and inductances in the circuit of Fig. 5 causes changes in its transfer function). However, these effects are not similar to the initial problem, only for the case of Fig. 10(j), which is very similar to Fig. 4(i), which states that for larger turn number in the ring coil (approaching to turn number of the planar coil), response to an input step voltage is the same as for any configuration. In this case, we see that these effects are due to the transfer function of the system, where we find that the double sine wave is seen only when the turn number ratio of the coils (planar coil vs ring coil) is between 15 and 25. When this relationship is not satisfied, the effect of the inductance and parasitic capacitances changes values in the terms of transfer function, eliminating this phenomenon of the double sine wave, what has been observed in other experiments realized with different turn numbers in planar coil.

5. CONCLUSION

This paper presents initial results of an experimental work, whose aim is to analyze phenomena generated by parasitic capacitance in coupled circuits formalized by a planar coil as the primary and a ring coil as the secondary. These phenomena present as not common by some numbers of turns in ring coil, when the primary (planar coil) is excited by a square wave of frequency between 1 kHz and 300 kHz, which is similar to the effect generated by an input step voltage. Observed phenomena show the existence of parasitic capacitances, but present a specific characteristic when number of turns of the secondary ring coil is reduced, having a specific pattern when the number is 9 and 10 turns, whose effect is quite noticeable. We can observe that this phenomenon occurs only when the input signal

is inserted in the center wire of the planar coil, with the ground as its edge. The found frequencies, when the number of turns is reduced, determine feasibility analysis of these effects over wires near inductances in circuits excited by square waves (as power electronics or computer systems) in electromagnetic interference analysis. Moreover, we observe that some specific phenomena are not observed when the circuit is inverted (planar coil as secondary and ring coil as primary), where the response does not show the frequency $f_{n<}$ that modulates the frequency $f_{n>}$ and the double exponential. However, another effect is presented, which is the elimination of symmetry of the response sine wave that is observed in ring coils with few turns, with the increased turn number in the ring coil. Also we note that the effect appears similar situation described in the first and second situations described above, when the turn number in the ring coil is approaching the turn number of the planar coil. We observe that main effect defined as double sine wave is verified only when the turn ratio of the coils is between 15 and 25, where the inductances and parasitic capacitances define values in transfer function that causes this phenomenon. Otherwise, the double sine wave is unverified, that is the same effect of inversion of the transformer; in this case, the values of inductances and parasitic capacitances change the transfer function, causing the same effect between Fig. 4 and Fig. 10 (the ratio between the turn number of coils is inverted).

REFERENCES

1. Oshiro, O., H. Tsujimoto, and K. Shirae, "A novel miniature planar inductor," *IEEE Transactions on Magnetism*, Vol. 23, No. 5, 3759–3761, September 1987.
2. Kaware, K., H. Kotama, and K. Shirae, "Planar inductor," *IEEE Transactions on Magnetism*, Vol. 20, No. 5, 1984–1806, September 1984.
3. Anioin, B. A., et al., "Circuit properties of coils," *IEE Proc. Sci. Mes. Technol.*, Vol. 144, No. 5, 234–239, September 1997.
4. Asdler, M. S., "A field-theoretical approach to magnetic induction of thin circular plates," *IEEE Transactions on Magnetism*, Vol. 10, No. 4, 1118–1125, December 1974.
5. Matsuki, H., N. Fujii, K. Shirakawa, J. Toriu, and K. Murakami, "Planar coil inductor with closed magnetic circuit," *IEEE Translation Journal on Magnetism in Japan*, Vol. 7, No. 6, 474–478, June 1992.
6. Matsuki, H., N. Fujii, K. Shirakawa, J. Toriu, and K. Murakami,

- “Arrangement of thin film cores for planar coil inductor,” *IEEE Translation Journal on Magnetism in Japan*, Vol. 8, No. 3, 177–181, March 1993.
7. Dudek, C., et al., “A new type of highly compact planar inductor,” *IEEE Transactions on Magnetism*, Vol. 43, No. 6, 2621–2623, June 2007.
 8. Kim, Y., F. Yang, and A. Z. Elsherbeni, “Compact artificial magnetic conductor designs using planar square spiral geometries,” *Progress In Electromagnetics Research*, PIER 77, 43–54, 2007.
 9. Yamada, S., et al., “Investigation of printed wiring board testing by using planar coil type ECT probe,” *IEEE Transactions on Magnetism*, Vol. 33, No. 5, 3376–3378, September 1997.
 10. Conway, J. T., “Noncoaxial inductance calculations without the vector potential for axisymmetric coils and planar coils,” *IEEE Transactions on Magnetism*, Vol. 44, No. 4, 453–462, April 2008.
 11. Wilcox, P. D., M. J. S. Lowe, and P. Cawley, “The excitation and detection of lamb waves with planar coil electromagnetic acoustic transducers,” *IEEE Transactions on Ultrasonics, Ferroelectrics, and Frequency Control*, Vol. 52, No. 12, 2370–2383, December 2005.
 12. Hurley, W. G. and M. C. Duffy, “Calculation of self- and mutual impedances in planar sandwich inductors,” *IEEE Transactions on Magnetism*, Vol. 33, No. 3, 2282–2290, May 1997.
 13. Castaldi, G., V. Fiumara, and I. Gallina, “An exact synthesis method for dual-band chebyshev impedance transformers,” *Progress In Electromagnetics Research*, PIER 86, 305–319, 2008.
 14. Chakravarty, T., S. M. Roy, S. K. Sanyal, and A. De, “Loaded microstrip disk resonator exhibits ultra-low frequency resonance,” *Progress In Electromagnetics Research*, PIER 50, 1–12, 2005.
 15. Grandi, G., et al., “Stray capacitances of single-layer solenoid air-core inductors,” *IEEE Transactions on Industry Applications*, Vol. 35, No. 5, 1162–1168, September/October 1999.
 16. Hole, M. J. and L. C. Appel, “Stray capacitance of a two-layer air-cored inductor,” *IEE Proc. Circuits Devices Syst.*, Vol. 152, No. 6, 565–572, December 2005.
 17. Marin, D., et al., “Modelling parasitic capacitances of the isolation transformer,” *In. Simpozionul National de Eletrotehnica Teoretica, SNET 2004*, Bucharest, October 2004.
 18. Yagashi, A., “Highly improved performance of a noise isolation transformer by a thin-film short circuit ring,” *IEEE Transactions on Electromagnetic Compatibility*, Vol. 41, No. 3, 246–250, August

- 1999.
19. Oshiro, O., H. Tsujimoto, and K. Shirae, "Structures and characteristics of planar transformers," *IEEE Translation Journal on Magnetics in Japan*, Vol. 4, No. 5, 332–338, May 1989.
 20. Rissing, L. H., S. A. Zielke, and H. H. Gatzen, "Inductive microtransformer exploiting the magnetoelastic effect," *IEEE Transactions on Magnetics*, Vol. 34, No. 4, 1378–1380, July 1998.
 21. Psarros, I. and I. Chremmos, "Resonance splitting in two coupled circular closed-loop arrays and investigation of analogy to traveling-wave optical resonators," *Progress In Electromagnetics Research*, PIER 87, 197–214, 2008.
 22. Su, Y. P., X. Liu, and S. Y. R. Hui, "Mutual inductance calculation of movable planar coils on parallel surfaces," *IEEE Transactions on Power Electronics*, Vol. 24, No. 4, 1115–1124, April 2009.
 23. Huang, Z., Y. Cui, and W. Xu, "Application of modal sensitivity for power system harmonic resonance analysis," *IEEE Transactions on Power Systems*, Vol. 22, No. 1, 222–231, February 2007.
 24. Cheng, K. W. E., et al., "Examination of square-wave modulated voltage dip restorer and its harmonics analysis," *IEEE Transactions on Energy Conversion*, Vol. 21, No. 3, 759–766, September 2006.
 25. Evans, P. D. and M. R. D. Al-Mothafar, "Harmonic analysis of a high frequency square wave cycloconverter system," *IEE Proceedings B*, Vol. 136, No. 1, 19–31, January 1989.
 26. Bailey, R. C., "The electrical response of an insulating circular disk to uniform fields," *Progress In Electromagnetics Research*, PIER 88, 241–254, 2008.
 27. Hussain, M. G. M. and S. F. Mahmoud, "Energy patterns for a conducting circular disc buried in a homogeneous lossy medium and excited by ultra-wideband generalized gaussian pulses," *Progress In Electromagnetics Research*, PIER 43, 59–74, 2003.
 28. Zhang, X., Y. Shi, and D. Xu, "Novel blind joint direction of arrival and polarization estimation for polarization-sensitive uniform circular array," *Progress In Electromagnetics Research*, PIER 86, 19–37, 2008.
 29. Besieris, I. and M. Abdel-Rahman, "Two fundamental representations of localized pulse solution to the scalar wave equation," *Progress In Electromagnetics Research*, PIER 19, 1–48, 1998.
 30. Ebine, N. and K. Ara, "Magnetic measurement to evaluate

- material properties of ferromagnetic structural steels with planar coils,” *IEEE Transactions on Magnetism*, Vol. 35, No. 5, 3928–3930, September 1999.
31. Tjossem, P. and V. Cornejo, “Measurements and mechanisms of Thomson’s jumping ring,” *Am. J. Phys*, Vol. 68, No. 3, 238–244, March 2000.
 32. Babic, S. and C. Akyel, “Improvement in calculation of the self and mutual inductance of thin-wall solenoids and disk coils,” *IEEE Transactions on Magnetism*, Vol. 36, No. 4, 1970–1975, July 2000.
 33. Good, R. H., “Elliptic integrals, the forgotten functions,” *Eur. J. Phys.*, Vol. 22, 119–126, 2001.